

Experimental Study on the Solidification of Heavy Metal Pb²⁺ in Fly Ash-based Geopolymers

Zirui Wang, Yiting Zhang *, Yahui Mao, Junchen Wu, Yifei Wang, Longhe Hu

School of Civil Engineering, Changchun Institute of Technology, Changchun, Jilin, 130012, China

* Corresponding author: Yiting Zhang (Email: zhangyiting@ccit.edu.cn)

Abstract

To promote the utilization of combustion by-products such as fly ash in green building materials and mitigate heavy metal pollution in the environment, fly ash-based geopolymers were prepared to immobilize lead ions (Pb²⁺). Systematic experiments were conducted to investigate the immobilization efficiency of fly ash-based geopolymers for Pb²⁺ and the mechanical properties of the geopolymer matrix. Furthermore, the microstructure of the geopolymer matrix and the intrinsic mechanism of Pb²⁺ immobilization were elucidated via X-ray diffraction (XRD), scanning electron microscopy (SEM), and Fourier transform infrared spectroscopy (FTIR). The results show that the optimal immobilization content of Pb²⁺ in fly ash-based geopolymers is 2.0% when both compressive strength and leaching concentration are taken into consideration. The immobilization of Pb²⁺ by fly ash-based geopolymers is achieved through the synergistic effects of chemical bonding and physical encapsulation.

Keywords

Fly Ash; Geopolymers; Heavy Metal Immobilization; Compressive Strength; Leaching Concentration; Microstructural Characterization.

1. Introduction

With the accelerated advancement of industrial modernization in China, heavy metal pollution from municipal solid waste and industrial solid waste has become an increasingly prominent environmental issue. These heavy metals can migrate into the soil-groundwater system via surface leaching and other pathways, posing severe threats to regional ecological security and human health. As a new type of inorganic cementitious material, geopolymers exhibit distinctive advantages in the solidification/stabilization of heavy metals owing to their unique three-dimensional aluminosilicate network structure[1]. Fly ash is a major industrial by-product generated from coal-fired power plants. Statistical data show that the cumulative stock of fly ash in China had reached 3.1 billion tons by 2021[2]. Featuring wide sources and low cost, fly ash is a promising raw material for preparing geopolymers for heavy metal immobilization. This approach can not only address the disposal dilemma of fly ash but also immobilize environmentally hazardous heavy metals, thereby realizing the goal of "treating waste with waste".

Pb²⁺ is a typical toxic heavy metal ion widely present in various solid wastes, which poses a substantial threat to the ecological environment and human health. Although numerous researchers have investigated the solidification/stabilization of Pb²⁺ using geopolymers, the underlying immobilization mechanism remains unclear and controversial. Van Jaarsveld et al. [3] proposed that Pb²⁺ could be chemically bonded within the aluminosilicate matrix, and heavy metal ions may alter the pore structure of cementitious materials. Leaching tests demonstrated that most Pb²⁺ cations are immobilized inside the matrix and cannot diffuse outward. Provis J.

et al. [4] found that a small amount of chromium migrates during the geopolymerization of fly ash-based geopolymers, and the use of water glass as an activator results in lower chromium migration compared with sodium hydroxide (NaOH) activation under high pH conditions.

In summary, heavy metal ions with different types and existing forms exert varying effects on the immobilization performance of geopolymers, and the corresponding immobilization mechanisms have not been fully elucidated to date[5-6]. Therefore, in this study, Pb^{2+} was introduced in the form of lead nitrate ($Pb(NO_3)_2$) to determine the optimal immobilization range and concentration of fly ash-based geopolymers for Pb^{2+} . The influence of Pb^{2+} content on the compressive strength of geopolymer solidified bodies was investigated, and the intrinsic immobilization mechanism of geopolymers for Pb^{2+} was revealed from a microstructural perspective.

2. Experimental Materials and Methods

2.1. Test Materials

Class I fly ash sourced from a coal-fired power plant in Jilin Province was used as the main raw material, whose XRD pattern, chemical composition, and SEM images are presented in Fig.1, Table 1, and Fig.2, respectively. Industrial water glass was supplied by Beijing Hongxing Guangsha Chemical Building Materials Co., Ltd. Analytical grade NaOH, $Pb(NO_3)_2$, ultrapure glacial acetic acid, and nitric acid were all purchased from Beijing Chemical Plant.

Table 1. Chemical composition of fly ash(wt%)

| SiO ₂ | Al ₂ O ₃ | Fe ₂ O ₃ | CaO | TiO ₂ | K ₂ O | MgO |
|------------------|--------------------------------|--------------------------------|------|------------------|------------------|------|
| 49.35 | 27.61 | 9.14 | 4.23 | 2.57 | 3.26 | 0.95 |

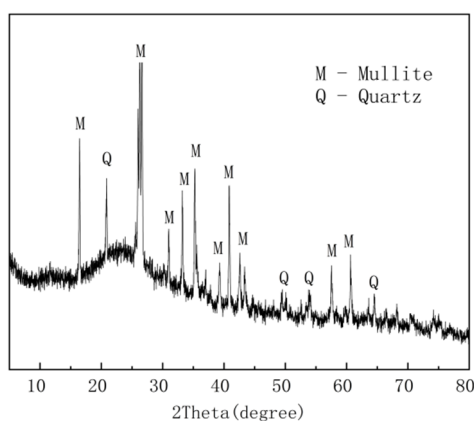


Fig 1. XRD pattern of fly ash

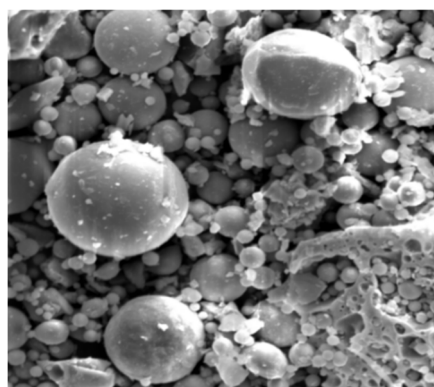


Fig 2. Fly ash SEM image

2.2. Preparation of Geopolymer Cured Bodies

Preliminary experiments were conducted to determine the optimal mix proportion of fly ash-based geopolymers, with a Si/Al ratio of 3.30, Na/Si ratio of 0.11, and water-binder ratio of 0.30. On this basis, different concentrations of Pb^{2+} were introduced into the geopolymer system. Table 2 lists the mix proportions of fly ash-based geopolymer solidified bodies with different Pb^{2+} contents.

Geopolymer specimens were prepared using a JJ-5 planetary cement mortar mixer according to the mix proportions in Table 2. Fly ash, alkaline activator (water glass and NaOH), deionized water, and $Pb(NO_3)_2$ solution were added to the mixer in sequence [7].

Table 2. Mix Proportion Material List for Fly Ash-Based Geopolymer Solidified Body

| Group | Fly ash/g | Water glass/g | NaOH/g | Water/g | Pb(NO ₃) ₂ /g | Pb ²⁺ Content/% |
|-------|-----------|---------------|--------|---------|--------------------------------------|----------------------------|
| 1 | 1000.00 | 299.17 | 47.80 | 104.94 | 8.00 | 0.50 |
| 2 | 1000.00 | 299.17 | 47.80 | 104.94 | 15.99 | 1.00 |
| 3 | 1000.00 | 299.17 | 47.80 | 104.94 | 23.99 | 1.50 |
| 4 | 1000.00 | 299.17 | 47.80 | 104.94 | 31.98 | 2.00 |
| 5 | 1000.00 | 299.17 | 47.80 | 104.94 | 39.98 | 2.50 |
| 6 | 1000.00 | 299.17 | 47.80 | 104.94 | 47.97 | 3.00 |

The mixture was stirred for a total of 3 minutes under programmed control (30 s at low speed → 60 s at high speed, repeated once). The prepared slurry was then poured into 40 mm×40 mm×40 mm polypropylene molds pre-coated with a release agent. The molds were vibrated on a vibrating table (50 Hz, amplitude 0.5 mm) for 120 s to eliminate air bubbles, and immediately sealed with polyethylene film to prevent moisture evaporation. The specimens were pre-cured at 25±2 °C for 2 h, then transferred to a high-temperature curing oven for thermal activation at 65 °C for 24 h. After demolding, the specimens were placed in a standard curing chamber (20±1 °C) for continuous curing until the designated ages of 3 d, 7 d, and 28 d. The prepared fly ash-based geopolymer specimens are shown in Figure 3. The specimens were taken out for compressive strength testing when reaching the preset curing ages.

**Fig 3.** Geopolymer solidified body based on fly ash

2.3. Mechanical Properties Testing

Compressive strength tests of the 40 mm×40 mm×40 mm non-standard cube specimens were carried out in accordance with the Chinese national standard GB/T 50081—2019 Standard for Test Methods of Mechanical Properties on Ordinary Concrete. The test was conducted in a standard environment of 20±2 °C: the cured specimens were loaded on a 2000 kN electrohydraulic servo testing machine with an accuracy grade of 0.5 at a loading rate of 0.2 MPa/s[8]. The measured strength values were corrected by a size effect factor to obtain the actual compressive strength of the specimens in accordance with the standard requirements.

2.4. Preparation and Testing of Leachate under Simulated Neutral and Acidic Environments.

Deionized water and a mixed acid solution of nitric acid and sulfuric acid were used as leaching agents to simulate the leaching behavior of Pb²⁺ from fly ash-based geopolymer solidified bodies into the soil under the action of surface water and acid rain during landfill disposal. The specimens after compressive strength testing at different curing ages were crushed for leaching tests. Leachates were prepared in accordance with HJ 557—2010 Solid Waste—Extraction Procedure for Leaching Toxicity—Horizontal Vibration Method and HJ/T 299—2007 Solid

Waste—Extraction Procedure for Leaching Toxicity—Sulfuric Acid & Nitric Acid Method. The leaching concentration of Pb^{2+} in the leachate was determined by inductively coupled plasma atomic emission spectrometry (ICP-AES) in accordance with relevant national standards. The test results are presented in Table 4 and Table 5.

3. Experimental Results and Analysis

3.1. Compressive Strength of Geopolymer Cured Body

Fly ash-based geopolymer solidified bodies with different Pb^{2+} contents (0.5%, 1.0%, 1.5%, 2.0%, 2.5%, and 3.0%) were prepared, and their compressive strengths at curing ages of 3 d, 7 d, and 28 d were tested. Table 3 shows the compressive strength test results of fly ash-based geopolymer solidified bodies with different Pb^{2+} contents [9]. To intuitively observe the strength variation and analyze its evolution law, the compressive strength of the solidified bodies with different Pb^{2+} contents is plotted as a line chart, as shown in Fig.4.

Table 3. Compressive Strength of Fly Ash-Based Geopolymer Specimens

| Group | Pb^{2+} Content/ % | 3d Compressive strength (percentage decrease in strength)/ MPa | 7d Compressive Strength (Percentage of Strength Reduction)/ MPa | 28d Compressive Strength (Percentage of Strength Reduction)/ MPa |
|-------|----------------------|--|---|--|
| 0 | 0.0 | 45.26 | 46.66 | 48.72 |
| 1 | 0.5 | 44.07(2.6%) | 45.73(2.0%) | 47.84(1.8%) |
| 2 | 1.0 | 42.96(5.1%) | 44.47(4.7%) | 46.67(4.2%) |
| 3 | 1.5 | 40.25(11.1%) | 41.99(10.0%) | 44.82(8.0%) |
| 4 | 2.0 | 37.54(17.1%) | 39.67(15.0%) | 42.39(13.0%) |
| 5 | 2.5 | 33.79(25.3%) | 36.86(21.0%) | 39.46(19.0%) |
| 6 | 3.0 | 27.38(39.5%) | 29.40(37.0%) | 31.67(35.0%) |

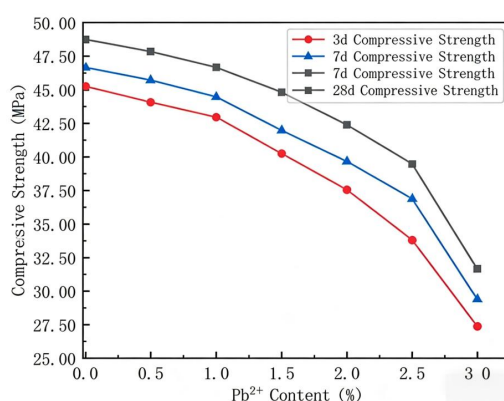


Fig 4. Trend of compressive strength of the solidified body with varying Pb^{2+} concentration

As shown in Fig.4, the compressive strength of fly ash-based geopolymer solidified bodies exhibits two distinct evolution characteristics: first, the mechanical properties of the specimens at all curing ages decrease gradually with the increase of Pb^{2+} content; second, the compressive strength of the solidified bodies increases significantly with the extension of curing age at the same Pb^{2+} concentration. Experimental data show that when the Pb^{2+} content is below 2.0%, the compressive strength of the specimens at 3 d, 7 d, and 28 d can still be maintained at approximately 40 MPa, and the strength loss rate is controlled within 17% compared with the

blank specimen without Pb^{2+} addition, demonstrating excellent mechanical stability[10]. When the Pb^{2+} content exceeds the critical value of 2.0%, the strength decay rate accelerates significantly. In particular, the 3 d compressive strength of the specimen with 3.0% Pb^{2+} content decreases by 39.5% compared with the blank specimen. Based on the systematic analysis of the evolution and attenuation characteristics of compressive strength with different Pb^{2+} contents, 2.0% is determined as the optimal immobilization concentration of fly ash-based geopolymers for Pb^{2+} from the perspective of mechanical properties.

3.2. Leaching Concentration of Heavy Metal Toxicity in Fly Ash-Based Geopolymer Solids

3.2.1. Leaching Results of the Powder Horizontal Oscillation Method (Simulating a Neutral Environment)

Table 4 presents the toxic leaching concentration of Pb^{2+} from fly ash-based geopolymer solidified bodies with different Pb^{2+} contents under simulated neutral environment, and the variation trend is shown in Fig.5.

Table 4. Toxic leaching concentration results corresponding to different Pb^{2+} concentrations in a neutral environment

| Group | Pb^{2+} Content/ % | Leaching concentration of heavy metals in solidified form(3d)/ $mg \cdot L^{-1}$ | Solidified heavy metals(7d)/ $mg \cdot L^{-1}$ | Solidified heavy metals(28d)/ $mg \cdot L^{-1}$ |
|-------|----------------------|--|--|---|
| 1 | 0.5 | 1.05 | 0.81 | 0.53 |
| 2 | 1.0 | 1.67 | 1.34 | 1.03 |
| 3 | 1.5 | 3.53 | 3.09 | 2.82 |
| 4 | 2.0 | 4.26 | 3.79 | 3.35 |
| 5 | 2.5 | 5.38 | 5.03 | 4.87 |
| 6 | 3.0 | 6.42 | 5.89 | 5.24 |

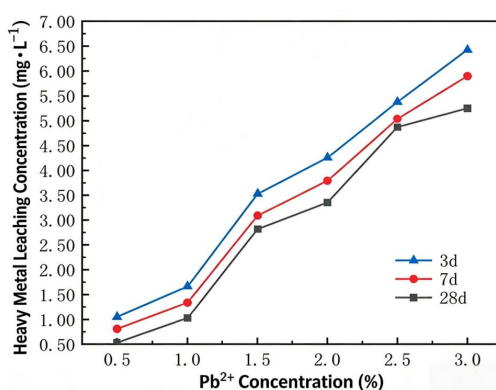


Fig 5. Trend chart of heavy metal toxicity leaching concentration in cured samples under neutral environment with changes in Pb^{2+} concentration

As shown in Fig.5, the Pb^{2+} leaching behavior of fly ash-based geopolymer solidified bodies under neutral environment is significantly correlated with the Pb^{2+} addition content. At the same Pb^{2+} concentration, the leaching concentration of Pb^{2+} decreases regularly with the extension of curing age, which is attributed to the gradual completion of the geopolymerization reaction inside the specimens and the formation of a dense cage-like network structure, which significantly enhances the immobilization capacity for heavy metal ions. When the Pb^{2+} content reaches 3.0%, the 3 d leaching concentration is $6.42 \text{ mg} \cdot \text{L}^{-1}$ and decreases to $5.24 \text{ mg} \cdot \text{L}^{-1}$ after 28 d of curing, slightly exceeding the national standard limit of $5 \text{ mg} \cdot \text{L}^{-1}$ with a limited excess

range. The Pb^{2+} leaching concentration increases stepwise with the increase of Pb^{2+} addition content; however, when the Pb^{2+} content is below 2.5%, the leaching concentrations at all curing ages can be stably controlled below the standard limit of $5\text{ mg}\cdot\text{L}^{-1}$. When the Pb^{2+} content exceeds 2.5%, the leaching concentrations of the specimens at 3 d and 7 d curing ages have exceeded the standard limit, while the 28 d leaching concentration first exceeds the limit when the Pb^{2+} content reaches 3.0%. Based on the correlation among toxic leaching concentration, curing age, and Pb^{2+} addition content, the optimal immobilization concentration range of fly ash-based geopolymers for Pb^{2+} is determined to be 2.0%–2.5% under neutral environment.

3.2.2. Leaching Results of the Sulfuric Acid-Nitric Acid Method (Simulating an Acidic Environment)

Table 5. Toxic leaching concentration results corresponding to different Pb^{2+} concentrations in an acidic environment

| Group | Pb^{2+} Content/ % | Leaching concentration of heavy metals in solidified mass(3d)/ $\text{mg}\cdot\text{L}^{-1}$ | Leaching concentration of heavy metals in solidified mass(7d)/ $\text{mg}\cdot\text{L}^{-1}$ | Leaching concentration of heavy metals in solidified mass(28d)/ $\text{mg}\cdot\text{L}^{-1}$ |
|-------|----------------------|--|--|---|
| 1 | 0.5 | 1.25 | 1.12 | 0.89 |
| 2 | 1.0 | 1.93 | 1.72 | 1.46 |
| 3 | 1.5 | 4.06 | 3.95 | 3.35 |
| 4 | 2.0 | 4.93 | 4.89 | 4.73 |
| 5 | 2.5 | 6.31 | 6.02 | 5.47 |
| 6 | 3.0 | 8.36 | 7.97 | 7.61 |

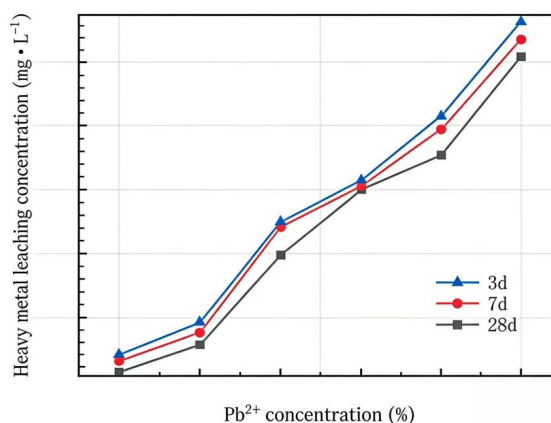


Fig 6. Trend of heavy metal toxicity leaching concentration in cured samples under acidic conditions with changes in Pb^{2+} concentration

As shown in Fig.6, a comprehensive analysis of the test data reveals that although the Pb^{2+} leaching behavior under acidic environment shares the same basic trend with that under neutral environment, the chemical erosion of acidic media significantly impairs the stability of the geopolymer solidified system. Under the continuous erosion of acidic leaching agents, the three-dimensional aluminosilicate network structure of geopolymers suffers from microcrack propagation and porosity increase, which makes it easier for Pb^{2+} to break through the encapsulation barrier of the geopolymer matrix and migrate outward. The test data show that at the same Pb^{2+} concentration, the leaching concentrations at all curing ages under acidic environment are 15%–28% higher than those under neutral environment, which confirms the significant negative effect of acidic pH on the immobilization efficiency of geopolymers for Pb^{2+} .

When the Pb^{2+} content reaches 2.0%, the leaching concentrations of the specimens at 3 d and 7 d curing ages are close to the standard limit of $5 \text{ mg}\cdot\text{L}^{-1}$, and the 28 d leaching concentration exceeds the limit when the Pb^{2+} content reaches 2.5%. Notably, the 7 d leaching concentration is slightly lower than the 3 d leaching concentration, while a significant decrease is observed from 7 d to 28 d. This phenomenon indicates that the geopolymer material has not fully exerted its chemical immobilization potential at 3 d of curing, and the continuous hydration and geopolymerization reactions from 7 d to 28 d make the solidified structure denser, thus the immobilization effect is further improved. The results show that the optimal immobilization concentration range of fly ash-based geopolymers for Pb^{2+} is still 2.0%–2.5% under acidic environment.

4. Study on the Mechanism of Pb^{2+} Solidification by Fly Ash-Based Geopolymers

4.1. X-ray Diffraction (XRD) Analysis

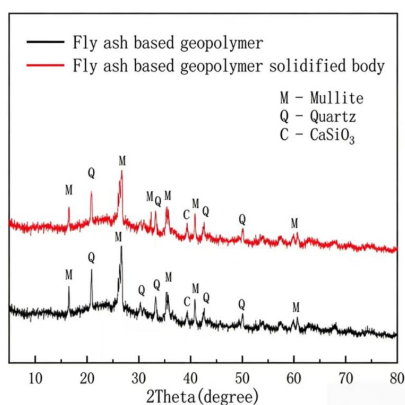


Fig 7. XRD Patterns of Fly Ash-Based Geopolymers and Their Cured Bodies

By comparing the XRD pattern of fly ash-based geopolymers (Fig.7) with that of raw fly ash (Fig.1), it can be seen that the main crystalline phases of fly ash-based geopolymers are still mullite and quartz, and a weak characteristic peak of calcium silicate ($CaSiO_3$) is detected at 39.54° . Compared with raw fly ash, the diffraction peak intensity of the crystalline phases in geopolymers is significantly reduced, which confirms that partial crystalline components are dissolved and transformed into amorphous gel products during the alkali activation reaction. The pure fly ash-based geopolymer exhibits a broad "hump-shaped" diffuse peak in the 18° – 35° 2θ range, and its peak position is slightly shifted to the right compared with that of raw fly ash, indicating that the dissolution of the glass phase in fly ash generates a large amount of amorphous aluminosilicate gel in the geopolymer system. For the geopolymer solidified bodies with Pb^{2+} addition, no characteristic peaks of lead-containing crystalline phases are observed in the XRD patterns, and the original crystalline phases of geopolymers do not disappear either. This indicates that Pb^{2+} does not participate in the chemical reaction to form new crystalline phases. Combined with the SEM microstructural analysis, it can be inferred that Pb^{2+} is immobilized in the geopolymer system through two pathways: on the one hand, Pb^{2+} is incorporated into the structural cavities of the geopolymer gel network in the form of ions to form chemical bonds; on the other hand, Pb^{2+} is physically encapsulated by the amorphous aluminosilicate gel matrix and residual crystalline particles, which restricts its migration and diffusion.

4.2. Scanning Electron Microscope (SEM) Analysis

To reveal the microstructural mechanism underlying the immobilization performance of fly ash-based geopolymers for Pb^{2+} , SEM tests were conducted on the pure fly ash-based geopolymer and its solidified bodies with different Pb^{2+} contents to analyze their micro-morphology and structural characteristics, as shown in Fig.8.

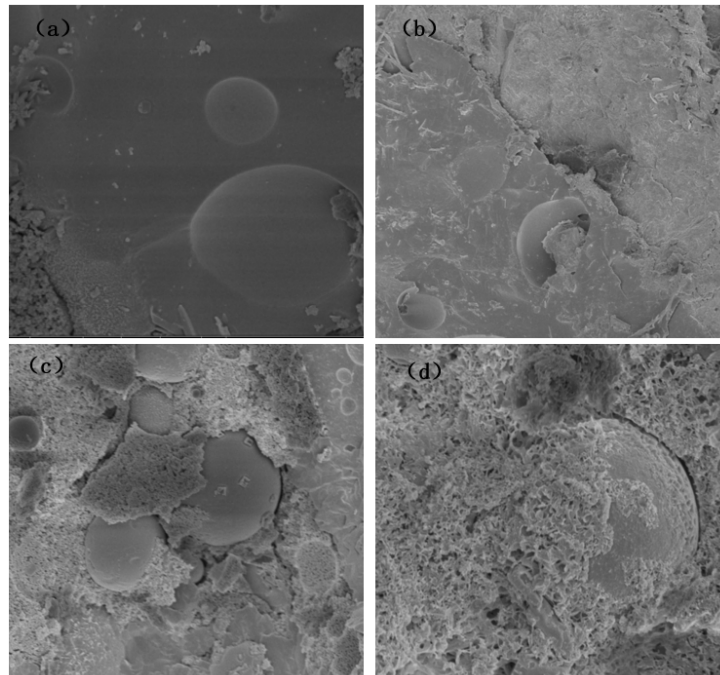


Fig 8. Scanning electron microscope image of the fly ash-based geopolymer Pb^{2+} solidified body

Fig.8(a) shows the SEM image of the pure fly ash-based geopolymer. It can be observed that after the alkali activation reaction, fly ash particles react completely to form a dense aluminosilicate gel matrix with a uniform, dense, and amorphous surface morphology. The original fly ash particles are either completely dissolved in the reaction process or encapsulated in the formed geopolymer gel, indicating that the depolymerization and polycondensation reactions inside the material proceed sufficiently and completely.

Fig.8(b) presents the SEM image of the geopolymer solidified body with 2.0% Pb^{2+} content. Compared with Fig.8(a), the incorporation of Pb^{2+} makes the microstructure of the geopolymer gel rougher and reduces the structural compactness. The interface between the fully reacted area and the partially reacted area is clearly observed in the image, which indicates that the introduction of Pb^{2+} inhibits the geopolymerization reaction to a certain extent.

Fig.8(c) and 8(d) are the SEM images of the geopolymer solidified bodies with high Pb^{2+} content. It can be seen that the internal structure of the specimens presents a loose flocculent morphology with a significant increase in pore volume and pore size. This phenomenon indicates that high concentrations of Pb^{2+} exert a strong inhibitory effect on the geopolymerization reaction, resulting in the formation of a loose internal structure. Such a microstructure leads to a significant decrease in compressive strength and a notable increase in Pb^{2+} leaching concentration of the geopolymer solidified bodies.

4.3. Infrared Spectroscopy (FTIR) Analysis

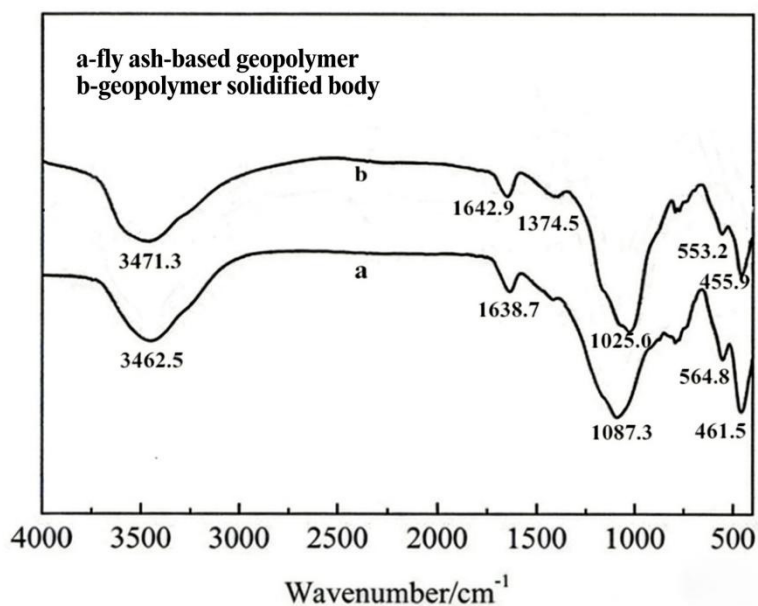


Fig 9. Infrared spectra of fly ash-based geopolymer and its cured body

As shown in Fig.9, the pure fly ash-based geopolymer (a) exhibits characteristic absorption peaks of O-H stretching vibration and O-H bending vibration at 3462.5 cm^{-1} and 1638.7 cm^{-1} , respectively; the geopolymer solidified body with Pb^{2+} (b) shows the corresponding absorption peaks at 3471.3 cm^{-1} and 1642.9 cm^{-1} , respectively. The slight shift of the absorption peaks is attributed to the presence of bound water in the geopolymer matrix and the hydrogen bonding interaction between Pb^{2+} and hydroxyl groups. The absorption peak at 1087.3 cm^{-1} for the pure geopolymer and 1025.6 cm^{-1} for the Pb^{2+} -immobilized geopolymer corresponds to the stretching vibration of Si-O-T (T = Si or Al) bonds in the aluminosilicate network. The significant shift of this absorption peak to the low wave number direction after the introduction of Pb^{2+} indicates that Pb^{2+} is incorporated into the aluminosilicate network framework of geopolymers and forms chemical bonds with the network structure. The absorption peaks at 564.8 cm^{-1} (pure geopolymer) and 553.2 cm^{-1} (Pb^{2+} -immobilized geopolymer) are assigned to the stretching vibration of Al-O-Si bonds, and the absorption peaks near 461.5 cm^{-1} (pure geopolymer) and 455.9 cm^{-1} (Pb^{2+} -immobilized geopolymer) correspond to the bending vibration of Si-O or Al-O bonds. A new absorption peak at 1374.5 cm^{-1} is observed only in the FTIR spectrum of the Pb^{2+} -immobilized geopolymer, which is attributed to the nitrate anions introduced by the $\text{Pb}(\text{NO}_3)_2$ additive [11]. In general, the FTIR spectra of the pure fly ash-based geopolymer and its Pb^{2+} -immobilized solidified body are basically consistent, with no significant changes in the positions of the main characteristic absorption peaks. This indicates that the introduction of Pb^{2+} only causes slight changes in the physicochemical properties of the geopolymer system, and the main structure of the geopolymer is still a complex three-dimensional network formed by the polycondensation of silicon-oxygen tetrahedra and aluminum-oxygen tetrahedra.

5. Conclusion

In this study, systematic experiments were conducted to investigate the Pb^{2+} immobilization efficiency of fly ash-based geopolymers and the mechanical properties of the corresponding solidified bodies. The microstructure of the geopolymer matrix and the intrinsic mechanism of Pb^{2+} immobilization was elucidated using XRD, SEM, and FTIR characterization techniques.

Based on the comprehensive analysis of the experimental results, the following conclusions are drawn:

- (1) From the perspective of compressive strength, the optimal immobilization concentration of fly ash-based geopolymers for Pb^{2+} is 2.0%. The compressive strength of the geopolymer solidified bodies decreases with the increase of Pb^{2+} content compared with the pure fly ash-based geopolymer, with the strength loss rate ranging from approximately 2% to 40%. This phenomenon indicates that Pb^{2+} exerts an inhibitory effect on the geopolymerization reaction and causes structural deterioration of the geopolymer matrix to a certain extent.
- (2) From the perspective of Pb^{2+} leaching concentration, the optimal immobilization concentration range of fly ash-based geopolymers for Pb^{2+} is 2.0%–2.5% under both neutral and acidic environments. At the same Pb^{2+} concentration, the leaching concentration of Pb^{2+} under acidic environment is significantly higher than that under neutral environment at all curing ages, which indicates that acidic media have a negative effect on the immobilization stability of geopolymers for Pb^{2+} .
- (3) Considering both compressive strength and Pb^{2+} leaching concentration comprehensively, the optimal immobilization concentration of fly ash-based geopolymers for Pb^{2+} is determined to be 2.0%. The performance evaluation of geopolymer solidified bodies for heavy metal immobilization is a multi-index comprehensive process, which requires strict control of heavy metal leaching concentration while ensuring a relatively high compressive strength. This is the key to promoting the engineering application of geopolymer solidified bodies in the field of heavy metal pollution control.
- (4) The combination of XRD, SEM, and FTIR characterization results reveals that the immobilization of Pb^{2+} by fly ash-based geopolymers is achieved through the synergistic effects of chemical bonding and physical encapsulation. On the one hand, Pb^{2+} is incorporated into the structural cavities of the aluminosilicate network framework and forms chemical bonds with the Si-O-T groups; on the other hand, Pb^{2+} is physically encapsulated by the dense amorphous aluminosilicate gel matrix, which restricts its migration and diffusion.

Acknowledgments

This work was supported by the 2025 Innovation and Entrepreneurship Training Program for College Students of Changchun Institute of Technology(S202511437138).

References

- [1] Jin Mantong. "Study on the Immobilization of Heavy Metals in Municipal Solid Waste Incineration Fly Ash Using Geopolymer" [D]. Nanjing University of Science and Technology, 2011.
- [2] Zhang Ningning, Shi Zhongyu, Han Rui, et al. "Research Progress on the 'Engineering-type' and 'Product-type' Utilization of Fly Ash" [J]. *Metal Mines*, 2022(5):26-36.
- [3] Van Jaarsveld J G S, Van Deventer J S J. "The effect of metal contaminants on the formation and properties of waste-based geopolymers" [J]. *Cement and Concrete Research*. 1999, 29(8): 1189-1200.
- [4] Provis J L, Rose V, Bernal S A, et al. "High-resolution nanoprobe X-ray fluorescence characterization of heterogeneous calcium and heavy metal distributions in alkali-activated fly ash" [J]. *Langmuir*. 2009, 25(19): 11897-11904.
- [5] Zhao Lijie, Zhang Tong, Huang Wei, et al. "Preparation and Properties of Coal Gasification Coarse Slag-Slag Based Geopolymers" [J]. *Bulletin of the Chinese Ceramic Society*, 2022, 41(10): 3542-3547.
- [6] He Zixiang, Luo Liting, Li Ruitao. "Study on the Properties of Polymer Mortar Based on Urban Municipal Solid Waste Incineration Fly Ash—Waste Glass Powder—Kaolin" [J]. *Chongqing Architecture*, 2025, 24(2): 58-63.

- [7] Bie R, Chen P, Song X, et al. "Characteristics of municipal solid waste incineration fly ash with cement solidification treatment" [J]. *Journal of the Energy Institute*. 2016, 89(4): 704-712.
- [8] He Chengyifeng. "Current Status and Suggestions on the Disposal Technology of Municipal Solid Waste Incineration Fly Ash under the New Situation" [J]. *Environment and Development*. 2019, 31(03): 66-67.
- [9] Wang Qikun, Ma Siqi, Yang Hualong, et al. "Research progress on the polymerization mechanism and kinetics of aluminosilicate polymers" [J]. *Journal of the Chinese Ceramic Society*, 2022, 50(9): 2551-2566.
- [10] Fang Haoyuan, Li Zhuowen, Jiang Shan, et al. "Study on the Proportioning of Slag-Kaolin Polymer Solidified Municipal Solid Waste Incineration Fly Ash" [J]. *Green Technology*, 2023(14): 184-187.
- [11] Silva RV, Brito JD, Lynn CJ, et al. "Environmental impacts of the use of bottom ashes from municipal solid waste incineration: A review" [J]. *Resources, Conservation and Recycling*, 2019, 140: 23-35.